

GEOREFERENCING OF EROS-A1 HIGH RESOLUTION IMAGES WITH RIGOROUS AND RATIONAL FUNCTION MODEL

F. Giulio Tonolo^a, D. Poli^b

^a DiGET, Politecnico di Torino, Corso Duca degli Abruzzi 24, 10129 Turin, Italy - fabio.giulionolo@polito.it

^b IGP, ETH Hoenggerberg, 8093 Zurich, Switzerland - daniela@geod.baug.ethz.ch

KEY WORDS: High resolution, Pushbroom, Georeferencing, Rigorous model, Rational Function Model, Eros A1.

ABSTRACT:

This paper investigates the potentials of strict and rational function models for the georeferencing of high-resolution images acquired by CCD linear array sensors. An image from EROS-A1 was oriented using both a strict sensor model for pushbroom sensors developed at ETH and a rational function model implemented at Politecnico of Turin.

The strict sensor model works with single images or two or more stereo images and is based on the classical collinearity equations; those equations are extended in order to include the sensor external orientation modeling, which is different for each image line, and the self-calibration. As the sensor external orientation concerns, the position and attitude are modeled with 2nd order piecewise polynomials depending on time (or line number, in case of constant scanning time), with constraints on the continuity of the functions and their first and second derivatives between adjacent segments. Additional pseudo-observations can fix the 2nd order parameters, resulting in a 1st order external orientation modeling. This option allows the modeling of the sensor position and attitude with 2nd or 1st order functions, according to the case study. The self-calibration is developed for the modeling of radial and decentering lens distortions, principal point/points displacement, focal length variation and CCD line rotation in the focal plane. The external orientation modeling and self-calibration are integrated into the collinearity equations. Using well-distributed Ground Control Points (GCPs), the external orientation and self-calibration parameters are estimated in a least-square adjustment. Using stereo images, Tie Points (TPs) can be added and their ground coordinates estimated. The initial approximations for the external orientation parameters are calculated by ephemeris, if available, or according to the satellite orbits.

The alternative proposed method, which is independent from the camera model and works on single images only, is the Rational Function Model (RFM). The 2D-image frame is related to the 3D-reference system on the ground through a ratio of 3rd degree order (maximum) polynomials, depending on 20 unknown coefficients. In order to estimate these coefficients it is necessary to collect from a minimum of 7 (1st order) to a maximum of 38 (3rd order) GCPs.

The two approaches have been applied to georeference a stereo pair acquired by EROS-A1 on 3rd February 2003. The scenes cover an area of approximately 12 x 19 km² over Caselle Airport (Turin), in Italy. A number of three dimensional GCPs have been identified in the image and measured in a 1:5,000 raster cartographic map. The satellite position at regular time instants was available from ephemeris recorded in the metadata file. This paper shows and discusses the accuracy obtained by the two methods.

1. INTRODUCTION

The georeferencing of remote sensing images is an important task for various remote sensing and photogrammetric applications, because it is an indispensable step for orthoimages generation and DEM production. Thanks to their large potentials, high-resolution sensors receive a great attention and can substitute aerial images acquisition in different applications (mapping, agriculture, forestry...).

Since the American authorities allowed the commercial marketing on space imagery of 1 meter and lately 0.5m resolution, the space high-resolution imagery market increased enormously and now provides a variety of high-resolution products.

Most of the high-resolution satellites use linear CCD arrays that scan the Earth surface in a pushbroom mode; in most cases they can also produce stereo images across- or along- the flight direction. The main advantage of along-track stereo geometry with respect to the across-track one is that the time delay between the stereo images acquisition is smaller. The along-track acquisition can be synchronous, if the satellite ground speed and the rate of imaging are equal, or asynchronous, if the satellite ground speed is faster than the rate of imaging.

The aim of georeferencing is to find a relationship between image and ground coordinates. In order to georeference images from CCD array sensors two different approaches, one parametric and one non-parametric, are used in the photogrammetric community.

The parametric (rigorous) models are based on the

photogrammetric collinearity equations and describe the exact acquisition geometry of CCD pushbroom sensors. By solving a bundle adjustment, the sensor external orientation and some additional geometric parameters are estimated (Ebner et al., 1992; Kornus, 1998; Kratky, 1989).

In the non-parametric approach the transformation between image and ground coordinates is represented by some general functions, without modeling the physical imaging process. Among the possible functions, the Rational Function Model (RFM) is widely used (Tao et al., 2001). It is based on the ratios of polynomials with different degree which can vary from 1 to 3. The coefficients are estimated using a large number of Ground Control Points (GCPs).

In this paper the georeferencing of EROS-A1 imagery with both RFM and rigorous model will be presented. The RFM has been implemented at DiGET, University of Turin, and the rigorous model at IGP, ETH Zurich. The results obtained from the two approaches are described and commented. Conclusions and future work will close the paper.

2. DATA

The images used in this study are two stereo scenes acquired by the Eros A1 satellite on the 3rd February 2003.

EROS-A1 was launched by ImageSat International (ISI) on the 5th December 2000 as first of a series of six high-resolution imaging satellites (Chen et al., 2002). In Standard Mode EROS-

A1 produces panchromatic images in the band of 500-900nm wavelength at 1.8m resolution, while the B1-B5 satellites will provide both panchromatic and multispectral imagery with better than 1m resolution. The satellite flies along a sun-synchronous near polar orbit at a height of 480km. As the instrument concerns, the NA30 camera on EROS-A1 is a high-resolution pushbroom sensor with 4 CCD arrays resulting in 7490 CCD elements; the scanning mode is asynchronous, therefore the satellite ground speed is faster than its rate of imaging.

ISI provides 3 different levels of images: 0A (raw scene), 1A (radiometrically corrected scene) and 1B (radiometrically and geometrically corrected scene). For our purposes, level 1A was chosen, because it preserves the original geometry of the acquisition.

The stereo images provided by ISI and used for our tests cover the test site of Caselle airport (Figure 1), in the outskirts of the city of Turin in Piedmont region (Italy). The images are about 19 km large and 12 km wide, with central latitude equal to 45.20N deg and central longitude equal to 7.66E deg.

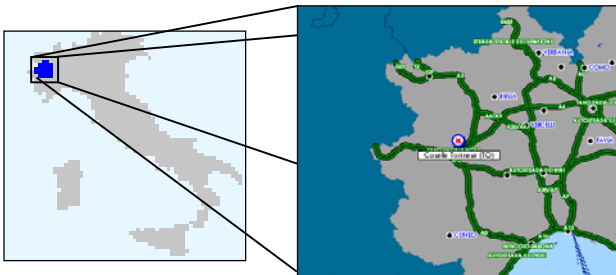


Figure 1. Test site location

The scenes have been acquired in along-track stereo mode with symmetric view angle and a ground resolution of about 2.6m (Figure 2).



(a)



(b)

Figure 2. Zoom of EROS-A1 stereo images over Caselle airport. A 50m x 50m grid Digital Elevation Model of the Piedmont Region with an accuracy of $\pm 5m$ was available, together with a raster 1:5,000 scale Technical Provincial Map (CTP) in Gauss-Boaga reference system. According to the expected scale mapping (which mainly depends on the geometric resolution of

the images) the CTP was used as cartographic reference.

The DEM and CTP were adopted to collect 13 GCPs over the stereo images (Figure 3) and 40 GCPs over a single image (Figure 4). The two groups of points were used for the images georeferencing with rigorous sensor model and RFM respectively. The points were measured in the images with manual matching (error of about 0.5 pixels).

In this paper the results obtained georeferencing one scene with RFM and the stereo pair with rigorous sensor model are presented.

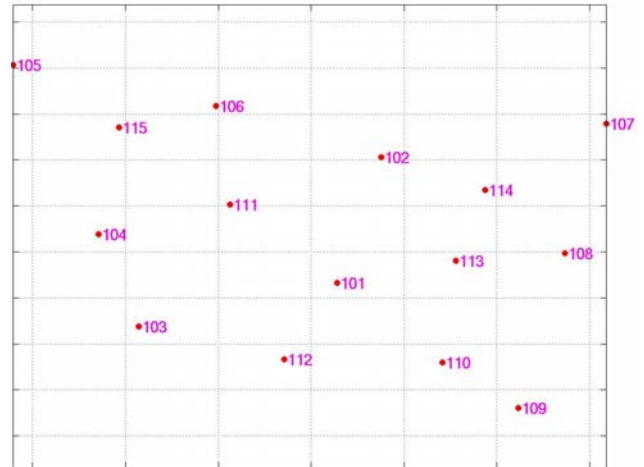


Figure 3. Distribution of 13 ground points used for the georeferencing of the stereo pair with rigorous sensor model.

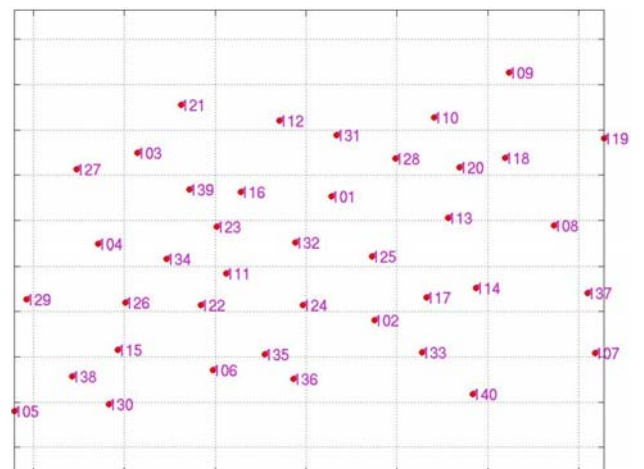


Figure 4. Distribution of 40 GCPs used to georeference one scene with RFM approach.

3. GEOREFERENCING WITH RFM

3.1 Model description

One of the most widely used non-parametric models is the Rational Function Model (RFM). This model, proposed by OPENGIS consortium, relates the two dimensional image coordinates (ζ, η) and the three dimensional terrain coordinates (X, Y, Z) through a ratio of polynomials P_i , as shown:

$$\begin{aligned}\xi &= \frac{P_a(X, Y, Z)}{P_b(X, Y, Z)} \\ \eta &= \frac{P_c(X, Y, Z)}{P_d(X, Y, Z)}\end{aligned}\quad (1)$$

P_i are usually third order maximum polynomials with 20 coefficients (a_0, a_1, \dots, a_{19}), i.e.:

$$\begin{aligned}P_a(X, Y, Z) &= a_0 + a_1X + a_2Y + a_3Z + a_4X^2 + \\ &+ a_5XY + \dots + a_{17}Y^2Z + a_{18}YZ^2 + a_{19}Z^3\end{aligned}\quad (2)$$

The previous equations are called RFM *upward equations*, because they allow the calculation of the image coordinates from the ground coordinates. The inverse transformation, that is the estimation of the terrain coordinates from the knowledge of the image coordinates and the Z values, can be performed according to the following equations, called RFM *downward equations*:

$$\begin{aligned}X &= \frac{P'_a(\xi, \eta, Z)}{P'_b(\xi, \eta, Z)} \\ Y &= \frac{P'_c(\xi, \eta, Z)}{P'_d(\xi, \eta, Z)}\end{aligned}\quad (3)$$

These non-parametric approaches based on Equations (1) and (3) has been developed at TU Turin in IDL programming language.

3.2 Polynomial coefficients estimation

In order to correctly estimate the polynomial coefficients in Equations (1) and (3) it is necessary to collect a sufficient number of GCPs. Considering that the first coefficient in the denominators is assumed to be equal to 1, the minimum number of GCPs to be collected ranges from 7 (1st order polynomial) to 39 (3rd order polynomial).

Equations (1) and (3) are linearized and written for each available GCP (N equations). Calling V the increment vectors, P the weight matrix, A the design matrix, L the observation vector and X the unknown vector, the system:

$$V = P \cdot A \cdot X - P \cdot L \quad (4)$$

is formed and solved with least-square solution:

$$X = (A^T \cdot P \cdot A)^{-1} \cdot A^T \cdot P \cdot L \quad (5)$$

where:

$$A^{(2N \times 78)} = \begin{pmatrix} \frac{\partial \xi_i}{\partial a_0} & \frac{\partial \xi_i}{\partial a_1} & \dots & \frac{\partial \xi_i}{\partial b_{19}} & 0 & 0 & \dots & 0 \\ \vdots & \vdots & \dots & \vdots & \vdots & \vdots & \dots & \vdots \\ 0 & 0 & \dots & 0 & \frac{\partial \eta_i}{\partial c_0} & \frac{\partial \eta_i}{\partial c_1} & \dots & \frac{\partial \eta_i}{\partial d_{19}} \end{pmatrix} \quad (6)$$

and:

$$\begin{aligned}X^{(78 \times 1)} &= \begin{pmatrix} a_0 - a_{0_{prev}} \\ \vdots \\ a_{19} - a_{19_{prev}} \\ b_1 - b_{1_{prev}} \\ \vdots \\ b_{19} - b_{19_{prev}} \\ c_0 - c_{0_{prev}} \\ \vdots \\ c_{19} - c_{19_{prev}} \\ d_1 - d_{1_{prev}} \\ \vdots \\ d_{19} - d_{19_{prev}} \end{pmatrix} & L^{(2N \times 1)} = \begin{pmatrix} \xi_i - \xi_{i_{prev}} \\ \vdots \\ \eta_i - \eta_{i_{prev}} \end{pmatrix} \\ & P^{(2N \times 2N)} = I & \text{at the 1st iteration}\end{aligned}\quad (7)$$

The Tikhonov regularisation algorithm (Tao et al., 2001) is applied in order to reduce the ill conditioning of the system (Equation 4). A small empirical coefficient (λ^2 , with $0.0001 < \lambda < 0.001$) is added to the diagonal elements of the $A^T P A$ (normal) matrix and the system in Equation 4 is rewritten as:

$$X = (A^T \cdot P \cdot A + \lambda^2 \cdot I)^{-1} \cdot A^T \cdot P \cdot L \quad (8)$$

where the identity matrix I has dimensions $N \times N$. This operation forces the system to converge after a few iterations.

Another problem is the occurrence of some asymptotes during the use of polynomials. An over parameterisation test was performed to evaluate which coefficients had to be used in the transformation. Firstly a χ^2 test ($\alpha=0.05$) was carried out to understand whether raw errors were present or whether the model was over-parameterised.

If over-parameterisation is detected, further analyses (*t Student* tests) are performed to identify the coefficients that can be neglected.

In order to force those coefficients to be null new equations are added to system in Equation (8) with a high weight.

It was found that both the number of coefficients to be used and the ill conditioning of the system are closely related to the geometric distortion due to the sensor attitude uncertainty and the elevation range of the scene.

3.3 Results

The presented model has already been used to perform position accuracy tests on other high-resolution sensors, like Quickbird (Borgogno, 2003b). In this study it was applied on one of the two stereo images. The scene has been georeferenced through the RFM in Gauss-Boaga refence system using the points distributed as in Figure 4. The scene was acquired in North to South direction with a forward viewing angle spanning from about 20° to about 40°.

The results of such processing have been evaluated through the accuracy evaluation of the planimetric positioning. Firstly the accuracy achieved on 40 GCPs used for the least square solution of the system 4 has been evaluated through statistical analysis on the residuals; then the same operation has been performed on 10 Check Points (CPs). Table 1 shows the accuracy test results.

	Mean dE (pixel)	Mean dN (pixel)	RMSE (pixel)	RMSE (m)
GCPs	0.104	0.042	0.27	0.70
CPs	0.838	0.565	1.94	5.04

Table 1. Accuracy test results with RFM.

The RMSE has been calculated according to the following

formulas:

$$RMSE = \sqrt{\frac{\sum_{i=1}^N RMS_i^2}{N-1}} \quad (9)$$

where:

$$RMS_i = \sqrt{dX_i^2 + dY_i^2} \quad (10)$$

dX_i and dY_i are the differences between correct and estimated ground coordinates.

The estimated parameters describing the *upwards* transformation, together with the DEM of the area, were used to rectify the image. Then the cartography at 10,000 scale was overlaid, resulting in the product showed in Figure 5.

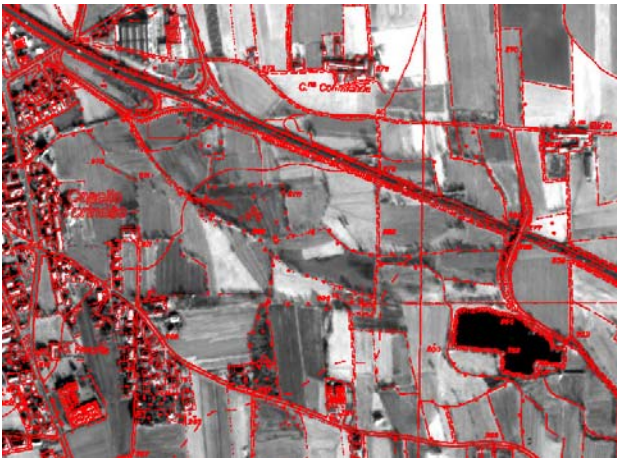


Figure 5. Rectified image with cartography.

4. GEOREFERENCING WITH RIGOROUS MODEL

4.1 Model description

The aim of rigorous sensor models is to establish a relationship between image and ground reference systems according to the sensor geometry and the available data. A flexible sensor model for the georeferencing of a wide class of linear CCD array sensors has been developed at IGP and already applied to different linear scanners carried on satellite and aircraft (Poli, 2003). The model is based on the photogrammetric collinearity equations. In fact each image line is the result of a nearly parallel projection in the flight direction and a perspective projection in the CCD line direction. Therefore for each observed point, the relationship between image and ground coordinates is described by the collinearity equations. The image system is centred in the lens perspective centre, with x -axis tangent to the flight trajectory, z -axis parallel to the optical axis and pointing upwards and y -axis along the CCD line, completing a right-hand coordinate system.

The model can be applied to single- and multi-lens sensors. In case of multi-line sensors, additional parameters describing the relative orientation (shifts and drifts) of each lens with respect to the central one are introduced. During the georeferencing of images from linear CCD array scanners, a particular attention must be addressed to their external orientation. In fact each image line is acquired with a different external orientation, that can not be estimated with a classical bundle adjustment, because the large number of unknowns (6 for each image line of each stereo image) would require an unrealistic number of GCPs. Then the sensor position and attitude are modeled with

suitable functions depending time (or line number). In our approach piecewise 2nd order polynomial functions depending on time are used. The platform trajectory is divided into segments according to the number and distribution of available GCPs and TPs. For each segment the sensor position and attitude are modelled by 2nd order polynomials and at the points of conjunction between adjacent segments constraints on the zero, first and second order continuity are imposed on the trajectory functions. Additional pseudo-observations can fix some or all parameters to suitable values. For example, if the 2nd order parameters are fixed to zero, the polynomial degree is reduced to 1 (linear functions). This option allows the modeling of the sensor position and attitude in each segment with 2nd or 1st order polynomials, according to the characteristics of the trajectory of the current case study.

In case of sensors carried on aircraft, additional GPS and INS observations can be included in the model (Poli, 2002).

The developed sensor model includes a self-calibration too, which is required for the correction of the systematic errors due to the lens (or lenses) distortions (principal point displacement, focal length variation, symmetric and decentering lens distortion) and the CCD lines rotations in the focal plane.

Finally the above-described functions modeling the external and the internal orientation are integrated into the collinearity equations, resulting in an indirect georeferencing model. Due to their non-linearity, the complete equations are linearized according to the first-order Taylor decomposition with respect to the unknown parameters. For this operation initial approximations for the unknown parameters are needed. The resulting system is solved with least square method.

An overview of the sensor model is given in Figure 4.

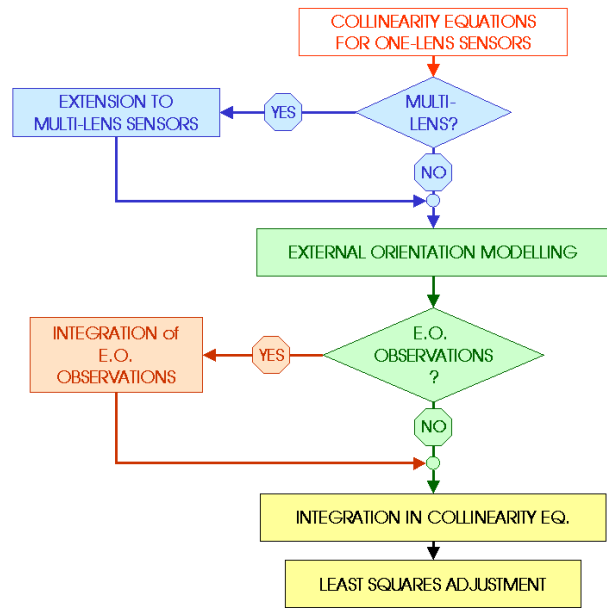


Figure 4. Overview of sensor model.

4.2 First results

The sensor model was applied to georeference the two stereo images over Caselle airport.

In this area 14 points measured in the images and on the ground were available. Figure 3 shows the points distribution.

The initial approximations of the sensor position at the time of acquisition of each image line were required. They were interpolated from the ephemerides contained in the image pass

file. The time of acquisition of each image line was calculated from the initial and final acquisition time of each image and the integration time (time of acquisition of each line).

The ephemerides consisted of the position and velocity in 4 time instants referred in ECI (Earth Centred Inertial) system, with X_{ECI} axis pointing to the vernal equinox, Z_{ECI} axis points to the celestial north pole and Y_{ECI} axis completing a right-hand coordinate systems. The ephemerides were transformed into the fixed Cartesian geocentric system. Then the satellite positions at the times of acquisition of each image line were calculated by interpolating the available measurements at 4 time instants with cubic splines.

Using the position rate of change available in metadata file the approximate values for the sensor attitude were also calculated. The sensor model was slightly changed in order to take into account a specific aspect of EROS-A1 geometry: the viewing angle is not fixed, but varies during the acquisition (pushbroom asynchronous). As no specific information was available, we supposed that the viewing angle rate of change was constant. Initial and final values were available from the images' metafile. The GCPs coordinates were transformed from Gauss-Boaga into Cartesian geocentric system and the georeferencing was performed in this system.

A group of available points were used as GCPs and the remaining as TPs. The RMS achieved on the TPs, which were computed by comparing the estimated ground coordinates of the TPs with the correct ones, were used as test control. Different tests were performed in order to decide the number and distribution of GCPs and TPs, the number of trajectory segment for the external orientation modeling, the polynomial degree and the parameters to estimate in the self-calibration.

About the external orientation modeling, there was not a considerable difference between using 2 or 4 segments for the piecewise functions, but the results were much worse if the polynomial degree was decreased from 2 to 1. Therefore the external orientation was modeled with 2 pieces of 2nd order polynomials. In this configuration, the stereo pair could be oriented using 8 well distributed GCPs. RMS of 3.347 m in X, 2.668 m in Y and 5.189 m in Z were obtained for the 8 GCPs and 4.806 m in X, 2.668 m in Y and 5.874 m in Z for the remaining 6 TPs. Considering the EROS-A1 ground pixel size of 2.8 m, the RMS of the TPs correspond to 1.65, 1.65 and 2.09 pixels in X, Y, Z.

The first results are satisfying, but they could be improved. First of all, as the distribution of the GCPs considerably influenced the sensor model performance, further tests are required, using a larger number of GCPs, TPs and CPs. Moreover the model could be adapted in order to include additional information about the complex EROS geometry acquisition. In this study the lack of information about the sensor internal orientation could be overcome with the self-calibration. In particular, the parameter that mostly affected the results was s_y , that is, the shear in y direction. This result is not surprising, because the asynchronous acquisition of EROS-A1 can produce such systematic effects.

5. CONCLUSIONS

In this paper imagery from EROS-A1 pushbroom sensor was georeferenced with RFM and strict sensor model. The results have been reported. The RFM was used on the single images, while the rigorous model was applied to the stereopair.

The planimetric accuracies obtained from the RFM approach were less than half pixel for the GCPs and about two pixel for the CPs.

The advantage of RFM model is that it is a general method

independent of sensor platform and can be applied on different sensors, without knowing the acquisition geometry.

Anyway the Rational Function Model is very unstable and its efficiency and accuracy depends on many factors, such as the distribution of the GCPs, the range of the elevation values, the sensor attitude and the Tikonov coefficient: all these parameters have to be evaluated for each single image. Poor estimations of these parameters can lead both to a decrease in the positioning accuracy and to the occurrence of asynthops in the final image (raw distortions).

The stereo pair georeferencing with the rigorous model was performed with 8 GCPs and a positioning accuracy of 1-2 pixels in the check points was achieved. These first results can be improved with a deeper investigation on the sensor acquisition geometry.

The work on EROS-A1 imagery needs more refinement. First of all, new points will be measured in the ground and in the images with sub-pixel accuracy in order to continue the tests and analyse the best input configuration.

Further developments of this study will be the evaluation of RFM based algorithms devoted to DTM extraction from stereo pairs images.

ACKNOWLEDGEMENTS

The rigorous sensor model development is part of Cloudmap2 project, funded by the European Commission under the Fifth Framework program for Energy, Environment and Sustainable Development.

The authors thank Enrico Borgogno, from DiGET (Turin) for his helpful collaboration.

REFERENCES

- Boccardo, P., Borgogno Mondino, E., Giulio Tonolo, F., 2003a, *Urban areas classification tests using high resolution panchromatic satellite images*, Urban 2003, Berlin (proceedings on CD).
- Boccardo, P., E. Borgogno Mondino, and F. Giulio Tonolo, 2003b. *High resolution satellite images position accuracy tests*. IGARSS 2003, Toulouse (proceedings on CD).
- Chen, L.C., Teo, T.-A., 2002. *Rigorous generation of digital orthophotos from EROS 1 high resolution satellite images*. International Archives of Photogrammetry and Remote Sensing, Vol. 34, Part B4, Ottawa, pp.620-625.
- Ebner, H., Kornus, W., Ohlhof, T., 1992. *A simulation study on point determination for the MOMS-02/D2 space project using an extended functional model*. International Archives of Photogrammetry and Remote Sensing, Vol. 29, Part B4, Washington D.C., pp. 458-464.
- Kornus, W., 1998. *Dreidimensionale Objektrekonstruktion mit digitalen Dreizeilenscannerdaten des Weltraumprojekts MOMS-02/D2*. DLR-Forschungsbericht 97-54 (in German).
- Kratky, V., 1989. *Rigorous photogrammetric processing of SPOT images at CCM Canada*. ISPRS Journal of Photogrammetry and Remote Sensing, No. 44, pp. 53-71.
- Poli, D., 2003. *Georeferencing of CCD linear array sensors imagery*. ASPRS Annual Meeting 2003. Anchorage, AK (USA) (proceedings on CD).
- Tao, C., Hu, Y., 2001, *A comprehensive study of the Rational Function Model for Photogrammetric processing*, Photogrammetric engineering & Remote Sensing, December 2001, pp.1347-1357.